Gut Microbes 4:4, 292–305; July/August 2013; © 2013 Landes Bioscience

Gut microbiota, tight junction protein expression, intestinal resistance, bacterial translocation and mortality following cholestasis depend on the genetic background of the host

Samuel M. Alaish,[1,*] Alexis D. Smith,[1] Jennifer Timmons,[1] Jose Greenspon,[1] Daniel Eyvazzadeh,[1] Ebony Murphy,[1] Terez Shea-Donahue,[2] Shana Cirimotich,[3] Emmanuel Mongodin,[3] Aiping Zhao,[2] Alessio Fasano,[2,4] James P. Nataro[5] and Alan Cross[2]

[1]Department of Surgery; University of Maryland School of Medicine; Baltimore, MD USA; [2]Department of Medicine; University of Maryland School of Medicine; Baltimore, MD USA; [3]Institute for Genome Sciences; University of Maryland School of Medicine; Baltimore, MD USA; [4]Department of Pediatrics; University of Maryland School of Medicine; Baltimore, MD USA; [5]Department of Pediatrics; University of Virginia School of Medicine; Charlottesville, VA USA

Keywords: cholestasis, intestinal microbiota, bacterial translocation, transepithelial electric resistance, bile duct ligation, interferon-gamma

Failure of the intestinal barrier is a characteristic feature of cholestasis. We have previously observed higher mortality in C57BL/6J compared with A/J mice following common bile duct ligation (CBDL). We hypothesized the alteration in gut barrier function following cholestasis would vary by genetic background. Following one week of CBDL, jejunal TEER was significantly reduced in each ligated mouse compared with their sham counterparts; moreover, jejunal TEER was significantly lower in both sham and ligated C57BL/6J compared with sham and ligated A/J mice, respectively. Bacterial translocation to mesenteric lymph nodes was significantly increased in C57BL/6J mice vs. A/J mice. Four of 15 C57BL/6J mice were bacteremic; whereas, none of the 17 A/J mice were. Jejunal IFN-γ mRNA expression was significantly elevated in C57BL/6J compared with A/J mice. Western blot analysis demonstrated a significant decrease in occludin protein expression in C57BL/6J compared with A/J mice following both sham operation and CBDL. Only C57BL/6J mice demonstrated a marked decrease in ZO-1 protein expression following CBDL compared with shams. Pyrosequencing of the 16S rRNA gene in fecal samples showed a dysbiosis only in C57BL/6J mice following CBDL when compared with shams. This study provides evidence of strain differences in gut microbiota, tight junction protein expression, intestinal resistance and bacterial translocation which supports the notion of a genetic predisposition to exaggerated injury following cholestasis.

Introduction

Cholestasis, defined as little or no flow of bile from the liver into the intestine, may be functional secondary to hepatic parenchymal disease, such as hepatitis, or mechanical due to an obstructing tumor or stricture. Regardless of the etiology, cholestasis, itself, produces an injury to not only the patient's liver but also their intestine. The genetic background of the host has long been known to be an important modifier of the inflammatory process associated with injury.[1] Studies using experimental murine models showed that inbred mouse strains displayed differences in the response to lipopolysaccharide (LPS).[2] A/J mice were found to be more resistant to LPS-induced mortality than other strains, with C57BL/6J (B6) mice being the most susceptible.[2] These observations were correlated with differences in the inflammatory response including the level of circulating TNF-α, IL-1β, Il-6 and the expression of acute-phase proteins in the liver.[2] Similar observations were made in a murine model of sepsis.[3]

Interestingly, A/J mice have also been found to be resistant toward *Salmonella* Typhimurium[4] and *Bordetella pertussis*[5] infections; however, A/J mice are susceptible to *Candida albicans*,[6] *Plasmodium chabaudi*,[7] *Listeria monocytogenes*,[8] and *Bacillus anthracis*.[9] In contrast, B6 mice are relatively resistant to each of these infections.[6-9]

Further analysis of these two mouse strains may uncover genetic variations responsible for disparate inflammatory responses after a different insult, such as common bile duct ligation (CBDL), which is a standard model for cholestasis.[10] Failure of the intestinal barrier is a characteristic feature of cholestasis, as bacteria from the intestinal lumen enter the circulation and/or initiate a systemic inflammatory response which can lead to

*Correspondence to: Samuel M. Alaish; Email: salaish@smail.umaryland.edu
Submitted: 11/16/12; Revised: 03/20/13; Accepted: 04/15/13
http://dx.doi.org/10.4161/gmic.24706

Table 1. Parameters tested which failed to show significant strain differences

Histology
Villus height, crypt depth and villus:crypt ratio
Degree of inflammation seen on hematoxylin and eosin slides of:
Intestine, liver, lung, kidney and heart
Apoptosis
Karyorrhexis and pyknosis
TUNEL assay for apoptosis

impairment of multiple organs. We have previously found differences in the systemic inflammatory responses and outcome following CBDL between two inbred mouse strains, C57BL6/cJ (B6) and A/J, suggesting a genetic contribution.[11] In particular, B6 mice were significantly more likely to develop ascites following one week of CBDL.[11] In concordance with this observation, the frequency of mortality after CBDL was significantly higher in B6 mice compared with A/J mice on days following CBDL.[11] Surprisingly, the liver chemistries and histology did not differ between the two strains of ligated mice. Each strain developed elevated serum bilirubin and transaminases as well as hepatic inflammation following CBDL.[11] Therefore, in this study, we have focused on the intestinal barrier in an attempt to begin to delineate the mechanism responsible for the different outcome between the two strains. Specifically, we examined tight junction protein expression, intestinal permeability and bacterial translocation following CBDL.

Increased permeability of the gut has been demonstrated in patients with inflammatory disorders such as Crohn disease[12-14] and cirrhosis[15,16] as well as animal models of intestinal inflammation and infection.[17-19] For example, cirrhotic rats with bacterial translocation have been found to have increased intestinal permeability.[20] Alterations in tight junction architecture are one cause of increased permeability.[21] Tight junction proteins can be occlusive in function such as ZO-1, claudin-1 and occludin, or they can be leaky in function, such as the pore-former, claudin-2. Changes in the expression of these different tight junction proteins alter the resistance of the intestinal barrier. Pro-inflammatory cytokines such as interferon-γ and tumor necrosis factor-α have been found to decrease epithelial barrier function by disrupting tight junction proteins in vitro.[21-25] Defined as the transmission of viable gut flora through the intestinal barrier, bacterial translocation has traditionally been determined by culture-positivity of mesenteric lymph nodes.[26] Bacterial translocation commonly occurs in both cirrhotic rats with ascites (45–78%) and cirrhotic patients.[27-29] We hypothesized that the genetic background modulates the intestinal barrier following cholestatic injury. Furthermore, we hypothesized differences in intestinal resistance and bacterial translocation account, at least in part, for the different outcomes in A/J and B6 mice following CBDL. We hypothesized that tight junction protein expression will vary by mouse strains, be altered by CBDL and directly correlate with mortality. Our data support these hypotheses. Moreover, our in vivo data implicates a well-published mechanism previously studied in vitro, the IFN-γ-mediated apoptosis-independent disruption of tight junction proteins.[21-25] Based on this study, human analysis would likely uncover similar genetic predispositions to cholestasis including single nucleotide polymorphisms.

Results

Histology and intestinal apoptosis following CBDL were consistent between mouse strains. One week following sham or CBDL operations, no significant differences were noted between the two strains in villus height, crypt depth or villus:crypt (V:C) ratio. The ligated mice exhibited dilated lymphatics and edema of the lamina propria; however, there were no differences in these phenotypes between the two mouse strains. Following three weeks of ligation, no strain differences were noted in the degree of inflammation present in the lungs, liver, kidneys and hearts of the mice.

There were no significant differences in apoptosis in intestinal crypt cells found between sham or ligated mice of either strain, nor were there any strain differences in apoptosis. The TUNEL assays both with and without pretreatment using diethyl pyrocarbonate (DPEC), which inhibits false positive staining due to endogenous nucleases, confirmed these negative findings. (**Table 1** summarizes parameters tested; data not shown).

Intestinal permeability varies with mouse strain. TEER was measured in the jejunum of B6 and A/J mice one week after CBDL or a sham operation. Following the sham operation, jejunal TEER was significantly lower in B6 mice compared with A/J mice ($p < 0.05$ by ANOVA), suggesting a higher baseline permeability in the B6 mice. Following CBDL, jejunal TEER was significantly reduced in each strain compared with their baseline (i.e., sham counterpart), ($p < 0.05$ by ANOVA); however, jejunal TEER was significantly lower in ligated B6 mice compared with ligated A/J mice ($p < 0.05$ by ANOVA) (**Fig. 1A**). A FITC-Dextran intestinal permeability assay performed simultaneously on sham A/J and B6 mice demonstrated increased permeability in the B6 mice as compared with the A/J mice, thus confirming the TEER results (**Fig. 1B**). In addition, intestinal resistance calculated from Ussing chamber measurements also confirmed decreased resistance in B6 as compared with A/J mice (**Fig. 1C**).

Bacterial translocation varies with mouse strain. Our pilot experiments demonstrated that a MLN-positive culture was a rare event after only one week of ligation. The paucity of translocation seen following one week of ligation was not totally unexpected, given how well-appearing were the mice. After three weeks of ligation, the vast majority of the mice showed signs of chronic obstructive jaundice including ascites. So, we studied this later time point. Three weeks following CBDL, MLNs from both strains were harvested and cultured on blood agar plates. Positive MLN cultures, a measure of bacterial translocation, were noted in four of 17 A/J mice (24%) vs. 10 of 15 B6 mice (67%) ($p = 0.03$). There was also a marked disparity in positive blood cultures; while four of 15 B6 mice (27%) were bacteremic, none of the 17 A/J mice were ($p < 0.05$). No significant differences were seen in liver and spleen cultures. In 12 of the 17 A/J mice, all of the cultures were negative; whereas, in only three of the 15 B6 mice were all of the cultures negative (**Table 2**). Interestingly, only one A/J mouse and two B6 mice had negative MLN cultures

but a positive blood, liver or spleen culture, suggesting that the route of translocation probably goes through the MLNs before the blood, liver or spleen. Bacteria isolated were predominantly aerobic gram-negative including *Enterobacter* and *Klebsiella*. *Enterococcus faecalis* and *Staphylococcus aureus* were also isolated. Positive cultures were rarely found in either mouse strain following the sham operation (1 of 11 A/J and 1 of 11 B6 mice).

In a mortality study, we confirmed our previous reported finding of increased mortality in B6 mice compared with A/J mice following CBDL. Three weeks after CBDL, seven of 13 B6 mice had died vs. 1 of 12 A/J mice ($p = 0.03$ by two-sided Fisher's exact test). One A/J mouse died from an anesthetic complication preoperatively and was therefore excluded from the analysis. Defining poor outcome as either death or a positive mesenteric lymph node culture in this study, 12 of 13 B6 mice (92%) had a poor outcome vs. 4 of 12 A/J mice (33%) ($p < 0.004$ by two-sided Fisher's exact test). Thus, B6 mice have greater rates of bacterial translocation and mortality following CBDL. This directly correlates with their decreased intestinal resistance and suggests a potential mechanism.

Soluble CD14 is markedly elevated in both strains of ligated mice compared with shams. A marker of monocyte response to LPS, soluble CD14 levels were dramatically increased in all mice 14 d following CBDL compared with shams ($p < 0.000002$), thus indicative of LPS translocation from the gut into the circulation. There was not a significant strain difference at this time point, which was not too surprising given that the mortality curves for the two strains do not begin to diverge until after the third postoperative week.[10]

Jejunal IFN-γ mRNA expression is increased in B6 compared with A/J mice. In an attempt to uncover pathways responsible for our above findings, we examined various cytokines and other mediators known to play a role in intestinal injury. One week following CDBL, jejunal tissue was collected from A/J and B6 mice. Q-PCR was used to examine the intestine for mRNA expression of the following: proinflammatory cytokines (IL-12a and b, IFN-γ), an anti-inflammatory cytokine (IL-10), cathepsin E, TLRs 2, 4 and 5, NODs 1 and 2 and the nuclear bile acid receptor, FXR (**Fig. 2**). Although the mRNA expression of TLR4, the ligand for LPS, was significantly decreased in ligated B6 mice compared with ligated A/J mice, the fold-change was less than 2 and probably of little physiologic significance, given the relatively low constitutive expression (threshold cycle of 28). However, IFN-γ mRNA expression was found to be 2- to 3-fold-increased in the jejunum of B6 mice compared with A/J mice ($p < 0.05$). This was true for sham-operated mice as well as ligated mice. This suggests that IFN-γ may play a role in the mechanisms contributing to the strain differences. Indeed, IFN-γ has been previously shown in vitro to disrupt epithelial barrier function by altering the architecture of the tight junction proteins, including a decrease in occludin expression.[21,23,24] Interestingly, we found that the B6 mice were deficient in cathepsin E in the intestine compared with A/J mice in sham-operated animals; however, that difference disappeared following CBDL (**Fig. 2**). IL-12b expression was significantly decreased in the B6 sham and ligated mice compared with their respective A/J counterparts (p

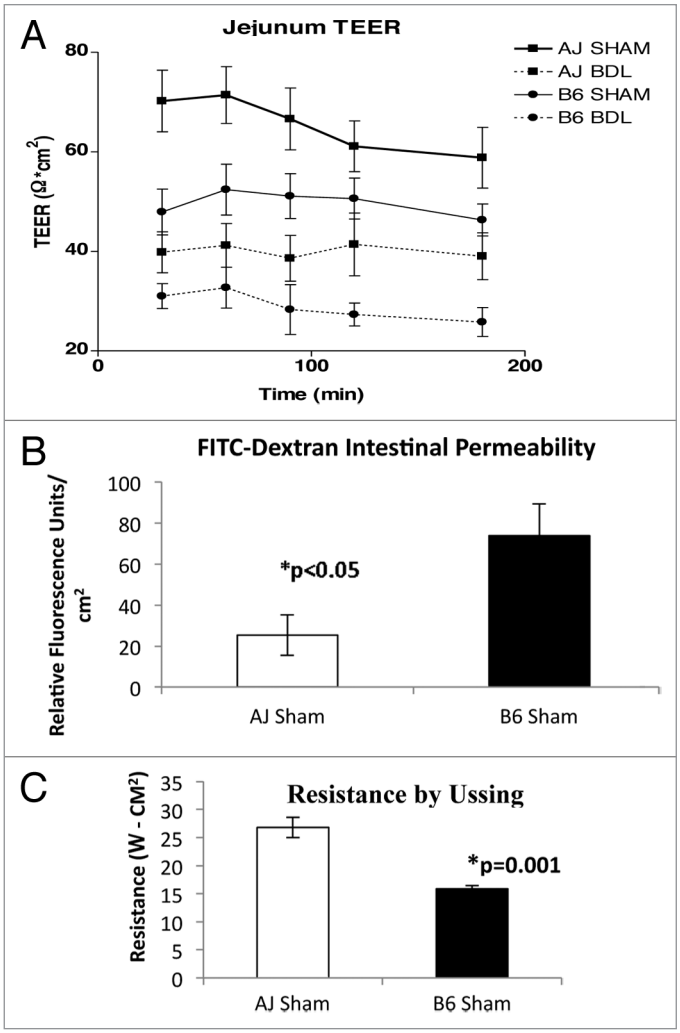

Figure 1. (**A**) Transepithelial electrical resistance (TEER) was measured ex vivo in jejunal specimens from sham and ligated A/J and B6 mice 7 d post-op. Measurements were taken at 30, 60, 90, 120 and 180 min following snapwell mounting. The epithelial permeability at 7 d was increased (TEER decreased) in B6 mice compared with A/J mice following sham operation (n = 8 sham A/J and 8 sham B6 mice). In addition, the epithelial permeability at seven days increased (TEER decreased) following CBDL in each strain (n = 8 CBDL A/J and 8 CBDL B6 mice). *$p < 0.05$ by ANOVA at every time point. (**B**) FITC-Dextran permeability assay results performed at the time of TEER confirm decreased intestinal barrier integrity in B6 mice compared with A/J mice, *$p < 0.05$. (**C**) Resistance calculated by Ussing chamber measurements confirm lower resistance in B6 mice compared with A/J mice, *$p = 0.001$.

Table 2. Incidence of bacterial translocation 21 d following CBDL

Incidence of bacterial translocation				
Strain	**MLN**	**B**	**L**	**S**
A/J	4/17	0/17	2/17	1/17
B6	10/15*	4/15**	2/15	3/15

Data are reported as # of animals with positive cultures per total animals of each strain. (MLN = mesenteric lymph node, B = blood, L = liver and S = spleen). *Positive MLN cultures were noted in 24% of A/J mice vs. 67% of B6 mice (Fisher's exact test, $p = 0.03$). **Whereas 27% B6 mice were bacteremic, none of the 17 A/J mice were (Fisher's exact test, $p < 0.05$).

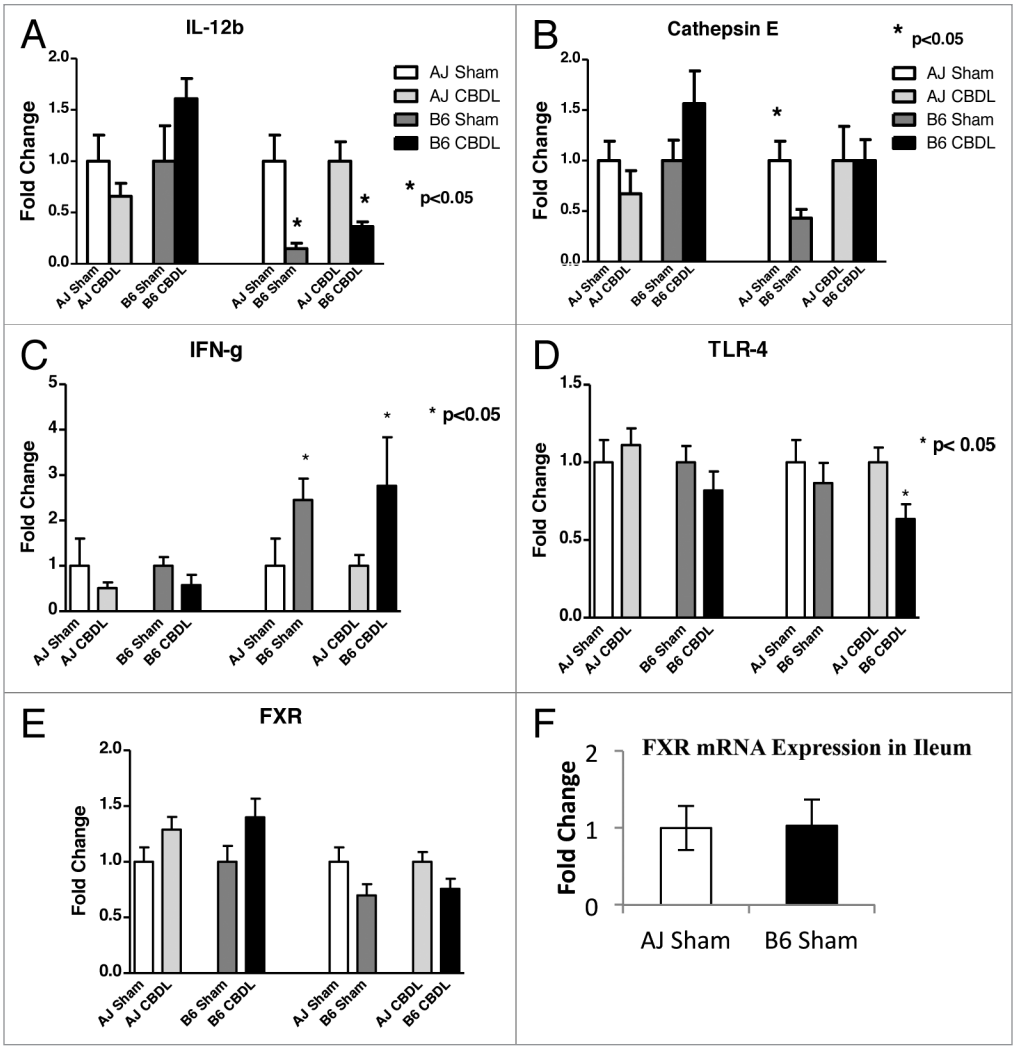

Figure 2. RT-PCR analysis of intestinal specimens collected on postoperative day 7 from sham and ligated A/J and B6 mice. Jejunal mRNA expression of IL-12b, Cathepsin E, IFN-γ and TLR4 had significant findings. Please note that for (**A**–**E**), the bar graphs provide four different comparisons of two bars each. For each pair of bars, the bar on the right has been normalized with respect to the bar on the left, which has been assigned a value of 1. (**A**) For IL-12b, there was a significant increase in ligated B6 mice compared with sham B6 mice. (**B**) For Cathepsin E, there was significantly greater expression in A/J sham mice compared with B6 sham mice. This difference disappeared following ligation. (**C**) IFN-γ mRNA expression was significantly elevated in both B6 sham and ligated mice compared with their A/J counterparts, *p < 0.05. (**D**) For TLR4, there was significantly less expression in ligated B6 mice compared with ligated A/J mice. n = 5 mice in each of four groups. (**E**) For FXR, there was no significant difference in jejunal expression between strains or following ligation. (**F**) FXR expression in the ileum did not vary between strains.

< 0.05). No strain differences were noted with respect to IL-12a (p35), IL-12b (p40), IL-10, TLR 2, TLR 5, NOD1, NOD2 or FXR mRNA expression (data not all shown).

Claudin-2 and occludin mRNA expression levels vary by mouse strain. The constitutive expression of each of the three tight junction proteins was noted to be quite high [threshold cycles of 20 (TJP-1), 21 (occludin) and 22 (claudin-2)]. The mRNA expression of a pore-forming tight junction protein, claudin-2, was increased in B6 mice compared with A/J mice. This was true for both sham (p = 0.035) and ligated (p = 0.015) animals. CBDL had no effect on claudin-2 mRNA expression; however, CBDL caused a pronounced decrease in the mRNA expression of an occlusive tight junction protein, occludin, in B6 mice (p = 0.005) (**Fig. 3**). There was a trend toward a decrease in occludin mRNA expression in ligated A/J mice compared with sham A/J mice (p = 0.07). No significant changes in TJP-1 (ZO-1) mRNA expression were found between strains or following CBDL. In summary, these alterations in the tight junction protein assembly may contribute to the decreased intestinal resistance previously noted in the B6 mice and play an early role in the cascade of events leading to the worse outcome found several weeks following CBDL in B6 compared with A/J mice.

Tight junction protein expression on western blots vary by genetic strain. Western blot analysis (**Fig. 4**) demonstrated a trend toward a decrease in occludin protein expression in B6 mice compared with A/J mice seven days following the sham operation (p = 0.10). No significant difference was found in either strain following the CBDL operation. B6 mice demonstrated a

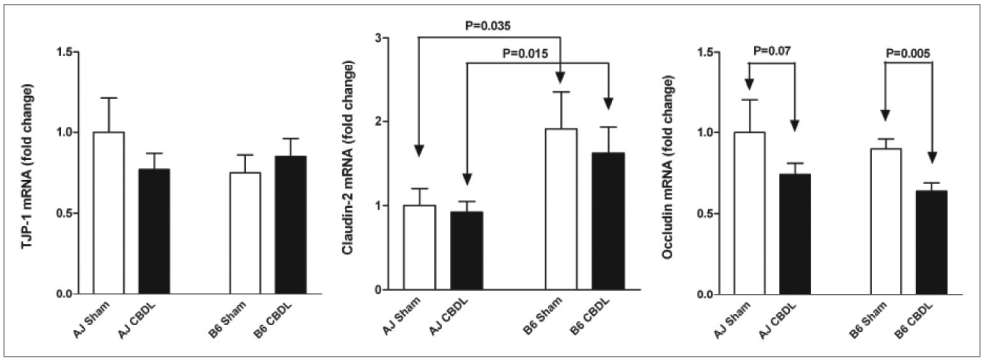

Figure 3. Jejunal tight junction protein mRNA expression in A/J and B6 mice 1 week following a sham or CBDL operation. Claudin-2 mRNA expression was increased in the B6 mice compared with the A/J mice; whereas, occludin mRNA expression was decreased in both strains following CBDL. No change was noted in TJP-1 (ZO-1) mRNA expression. n = 5 in each of four groups.

marked decrease in ZO-1 protein expression following CBDL compared with shams (*p < 0.0002); whereas, there was no significant change in ZO-1 protein expression in A/J mice following CBDL. Claudin-1 protein expression was significantly decreased in ligated B6 mice compared with B6 shams (*p < 0.02) but no significant change was found in the A/J strain. Interestingly, claudin-2 protein expression was also decreased in B6 sham mice compared with A/J sham mice (*p < 0.05). There was a trend toward decreased claudin-2 expression in ligated B6 mice compared with ligated A/J mice (p = 0.09).

Increased mortality following CBDL in IFN-γ $R^{-/-}$ mice compared with wild-type mice is not seen in C57BL/6J IFN-$\gamma^{-/-}$. Previously, Sewnath et al.[34] demonstrated that endogenous IFN-γ was protective against cholestatic liver injury. They showed that IFN-γ receptor $(R)^{-/-}$ mice had a much lower survival (40% mortality) 2 weeks following CBDL than the wild-type 129/Sv mice (0% mortality). Moreover, the IFN-γ $R^{-/-}$ mice had more severe jaundice and cholestatic liver injury reflected by higher serum bilirubin and liver enzyme levels as well as histology. Given our previous finding of increased IFN-γ expression in the intestine of B6 mice, we hypothesized that IFN-$\gamma^{-/-}$ C57BL/6J mice would have increased intestinal resistance compared with wild-type C57BL/6J mice following CBDL, which would impact survival. Following 2 weeks of CBDL, 0% mortality was observed both in the wild-type C57BL/6J mice and IFN-$\gamma^{-/-}$ C57BL/6J mice, p = NS (**Fig. 5**). This is in stark contrast to the 40% mortality previously seen in the IFN-γ $R^{-/-}$ mice.[32] Despite its protective role to the liver, IFN-γ may be simultaneously damaging to the intestine during the complex pathologic condition of cholestasis.

Gut microbiota displays a dysbiosis following CBDL in B6 but not A/J mice. Qualitative changes in the gut microbiota were assessed by massively parallel pyrosequencing, because conventional culture techniques fail to culture the majority of bacteria. We found a significant change in the microbiota in the B6 mice 14 d following CBDL compared with shams. This dysbiosis was not seen in the A/J mice (**Fig. 6**). Therefore, the intestinal dysbiosis observed is positively correlated with the strain-dependent later increase in mortality following CBDL in mice. The Principal Coordinates Analysis (PCoA) demonstrates tight clustering of the bacterial community for the ligated B6 mice which is separate from the tight clustering of the bacterial community for the sham B6 mice. On the other hand, both the sham A/J

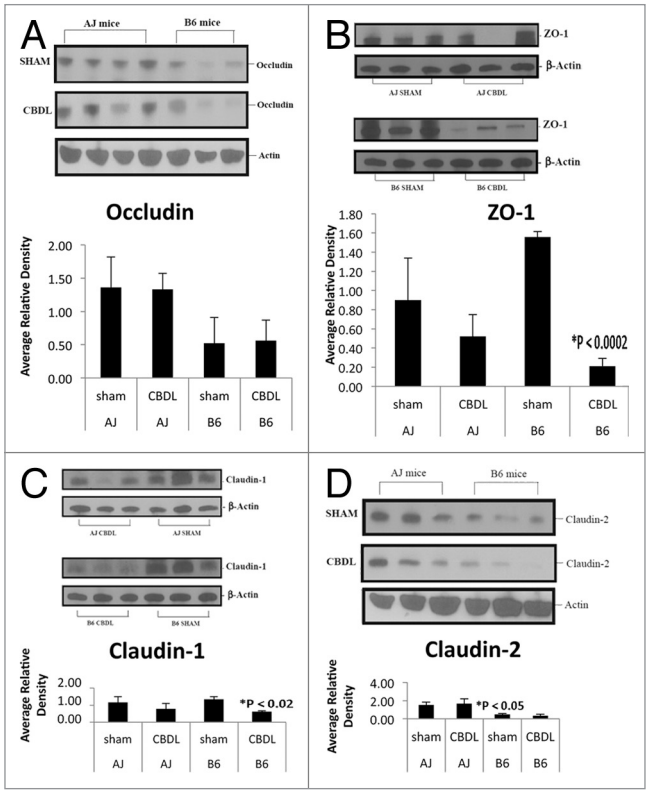

Figure 4. Tight junction protein expression by western blot analysis. Note each lane represents tissue from a separate mouse. (**A**) Occludin protein expression appeared decreased in B6 mice compared with A/J mice; however, densitometry showed only a trend when comparing shams (p = 0.10). (**B**) Following CBDL, ZO-1 protein expression was significantly decreased in B6 mice (*p < 0.0002) but not A/J mice. (**C**) Claudin-1 protein expression decreased significantly (*p < 0.02) in B6 but not A/J mice following CBDL. (**D**) Interestingly, claudin-2 protein expression was significantly decreased in B6 sham mice compared with A/J sham mice (*p < 0.05). There was a trend toward decreased claudin-2 expression in B6 CBDL mice compared with A/J CBDL mice (p = 0.09).

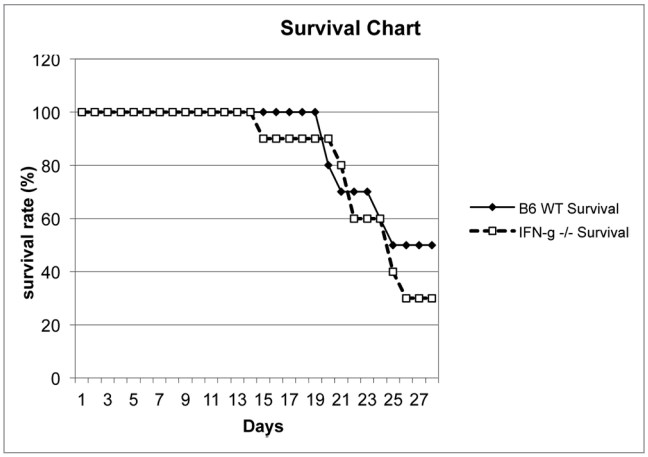

Figure 5. Survival graph following CBDL in IFN-$\gamma^{-/-}$ (C57BL/6J background) (n = 10) and wild-type C57BL/6J (B6) (n = 10) mice. No significant difference in mortality was found at any time point out to four weeks.

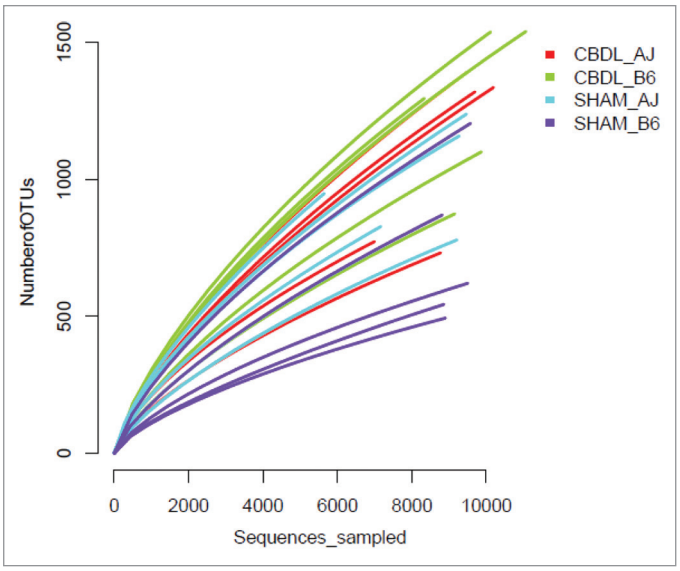

Figure 6. Rarefraction curves for fecal microbiota collected from sham and ligated A/J and B6 mice (n = 5 mice for each of four groups). The number of species is plotted against the number of samples analyzed.

and ligated A/J mice display similar bacterial communities with considerable overlap (**Fig.** 7). The *Firmicutes*:*Bacteroidetes* ratio was significantly elevated in the B6 mice compared with the A/J mice (**Fig. 8**). No effect on this ratio was apparent following CBDL; however, there was a marked decrease in the relative amount of *Lactobacillus* organisms and a great increase in the relative number of clostridial organisms along with a small increase in the relative number of proteobacterial organisms in the B6 mice following CBDL as compared with their sham counterparts (**Figs. 9 and 10**). No relative increase in either clostridial or proteobacterial organisms was found in the ligated A/J mice.

Additional statistical analyses of the microbiota were performed. The number of observed operational taxonomic units (OTUs) increased significantly in B6 mice following CBDL compared with shams; however, no significant difference was seen in A/J mice following CBDL compared with shams (**Fig. 9**). The bacterial diversity was significantly increased in the B6 mice following CBDL compared with shams as determined by the Shannon diversity index (**Fig. 10**). No significant difference was noted in the A/J strain. Similarly, bacterial richness was significantly increased in the B6 mice following CBDL compared with shams as determined by the Chao1 richness estimate (**Fig. 11**).

Discussion

Both the systemic inflammatory response and mortality following CBDL have previously been shown by our laboratory to vary with the genetic inbred strain when studied in a mouse model.[11] This suggested that some differences in the genetic background may affect the inflammatory response seen following CBDL. The findings from this study not only confirm the mortality observation, but also provide in vivo support for a potentially responsible mechanism, the IFN-γ-mediated mechanism of tight junction disruption, which has already been well-characterized in vitro.[21-25]

The modified "Snap-well" assay pioneered by El Asmar et al.[31] and used in this study is a quick and reproducible method to measure TEER in tissue. Decreased TEER correlates with increased permeability and has been described in mouse models in the setting of intestinal infections, including *Giardia lamblia*,[18] *Campylobacter jejuni*,[35] *Salmonella* Typhimurium,[36] and enterohemorrhagic *Escherichia coli* O157:H7.[37] We found decreased TEER in the small intestines of both A/J and B6 mouse strains following CBDL, which is in agreement with others who have found increased intestinal permeability following CBDL in mice.[38] A novel finding in this study was that B6 mice had decreased jejunal TEER after a sham operation compared with A/J mice, as well as decreased jejunal TEER following CBDL compared with ligated A/J mice; however, the "net" decrease in TEER in each strain following ligation appeared similar. Therefore, it may well be that the sham or "baseline" TEER in the B6 mice is so low that following the ligation, a pathologic threshold is crossed.

Given that the mice underwent the same insult and were housed under identical environmental conditions, the difference in their genetic backgrounds is implicated but not proven; there remains the confounding variable of the effects of the intestinal flora. It is well documented that both the type and concentration of bacteria present in the intestinal lumen affects intestinal barrier function.[39] Certain types of bacteria such as *Escherichia coli* translocate in large numbers from the intestinal tract to the draining mesenteric lymph nodes; gram-positive bacteria translocate at intermediate levels, and anaerobic bacteria translocate at very low levels.[39] In addition, intestinal permeability is increased with bacterial overgrowth.[39] An additional caveat is that kinship has been shown to be a significant determinant of the intestinal microbiota.[40] Consequently, the intestinal flora may not be an exclusive environmental factor but may, itself, have a genetically

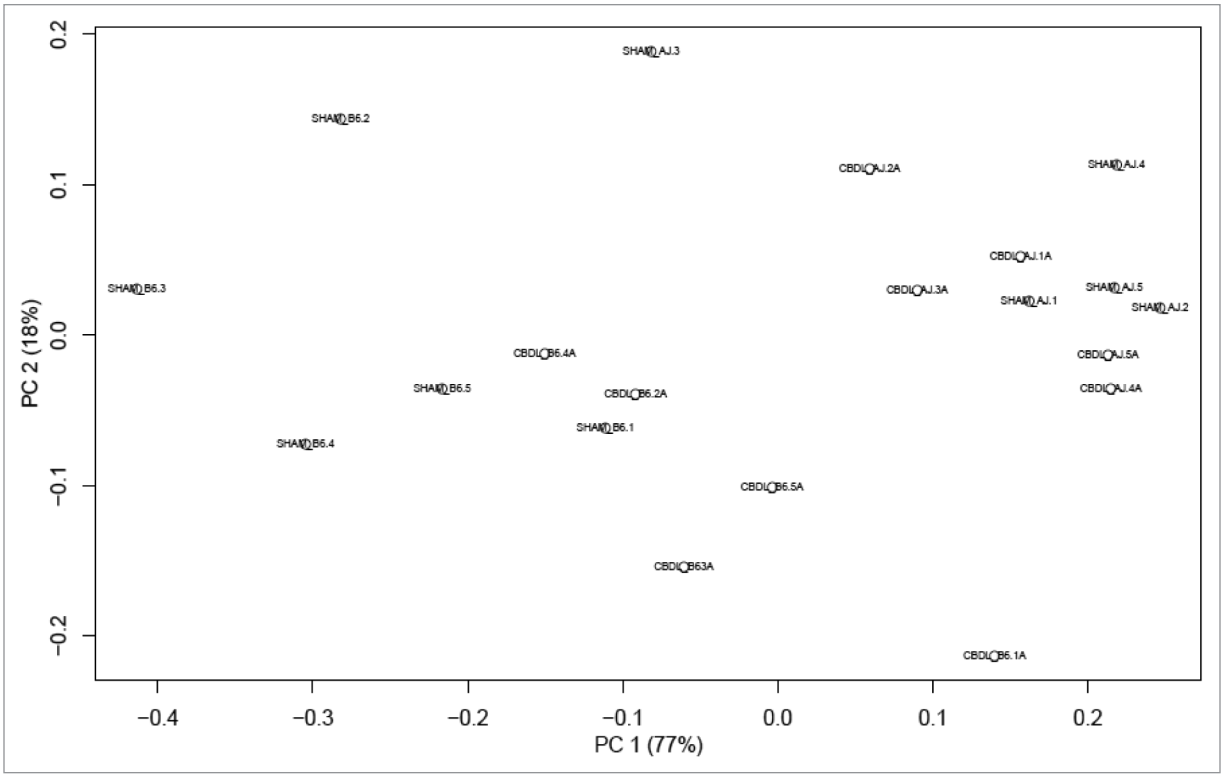

Figure 7. Principal coordinates analysis (PCoA) plot of fecal microbiota collected from sham and ligated A/J and B6 mice (n = 5 mice for each of four groups). This analysis enables visualization of similarities of the microbiota data. Three separate clusters can be seen: ligated B6 mice, sham B6 mice and A/J mice (both sham and ligated).

determined component. Our findings support this statement. Despite identical environmental conditions, including diet, the B6 mice had different bacterial communities compared with the A/J mice. There were 3 distinct clusters on our PCoA graph: B6 sham, B6 CBDL and A/J (CBDL and Sham). The distinct B6 sham cluster suggests that the baseline microbiota differs between the B6 and A/J strains. We speculate that this difference in the microbiota is then responsible for the different baseline intestinal resistances, for it has been shown that changes in the gut microbiota lead to changes in the intestinal resistance.[38] Hence, the ligated B6 mice displayed a dysbiosis which was not seen in the ligated A/J mice. This finding differs from a recently published article[41] which failed to show a dysbiosis in B6 mice 10 d following CBDL; however, 50% of the bacteria in that study could not be identified. Bacterial diversity and richness statistical analyses confirmed the gut microbiota in B6 mice following CBDL to be more complex than in their sham counterparts. This result along with an increased *Firmicutes*:*Bacteroidetes* ratio in the B6 mice as compared with the A/J mice might contribute to the decreased intestinal resistance, increased bacterial translocation and increased mortality later seen in the B6 mice following CBDL. An increased *Firmicutes*:*Bacteroidetes* ratio has been associated with both genetically-induced[40,42] and high fat-diet-induced obesity in mice.[43] Moreover, ZO-1 mRNA expression was shown to be decreased and endotoxemia to be increased in mice fed a high-fat diet, and this positively correlated with inflammatory markers, oxidative stress and macrophage infiltration markers.[44,45] We

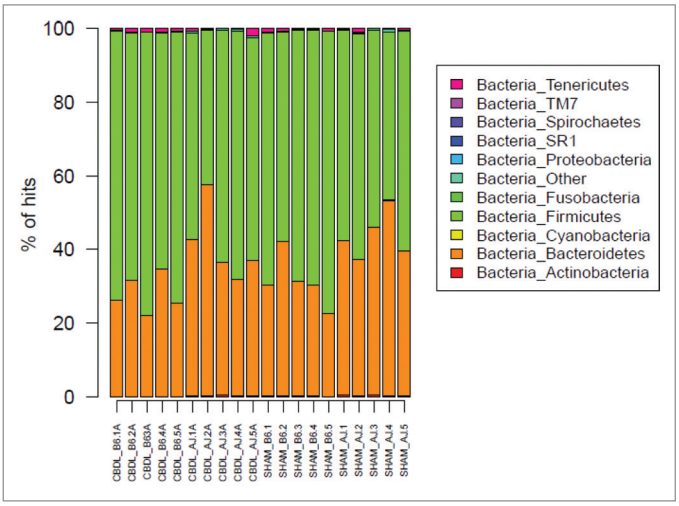

Figure 8. Bar graph of phyla for fecal microbiota from sham and ligated A/J and B6 mice (n = 5 mice for each of four groups). Firmicutes and Bacteroidetes dominate the phyla of both strains; however, note the increased *Firmicutes*:*Bacteroidetes* ratio in the B6 as compared with the A/J mice.

speculate that the B6 mice may be more likely to develop chronic systemic inflammation because of their relatively increased numbers of *Firmicutes* compared with *Bacteroidetes*. The relative increase in the number of both clostridial and proteobacterial

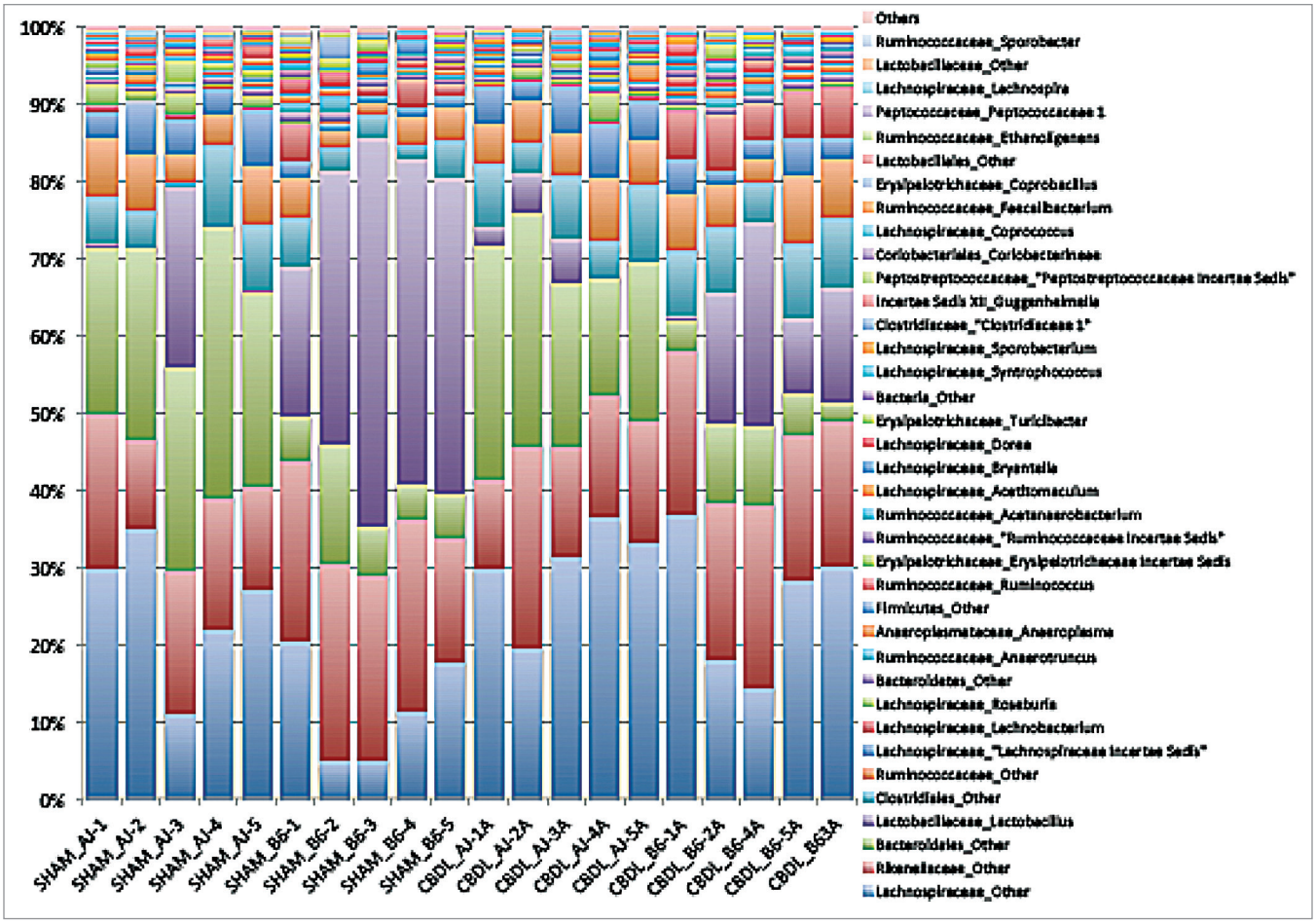

Figure 9. Bar Graph of genera for fecal microbiota collected from sham and ligated A/J and B6 mice (n = 5 mice for each of four groups). Note the decrease in *Lactobacillus* (first purple bar from the bottom) and increase in *Clostridiales* (blue bar directly above first purple bar from the bottom) in ligated B6 mice as compared with sham B6 mice. This signifies a transition from a more benign to a more virulent microbiota.

organisms and relative decrease in *Lactobacillus* in the ligated B6 mice compared with their sham counterparts may be indicative of a transition toward a more pathogenic microbiota which three weeks later contributes to the significant mortality difference between the strains.[10] Both Clostridia and Proteobacteria have each been recently shown to be increased in the gut microbiota in a preterm piglet model of necrotizing enterocolitis[46] as well as in premature infants with this disease.[47]

Increased bacterial translocation in mice following CBDL has been previously described.[48,49] Our results not only confirm but expand this finding. Different strains of inbred mice were found to have a different incidence of bacterial translocation to both MLNs and the bloodstream following CBDL. Increased septic complications in cholestatic patients are thought to be due to the failure of the intestinal barrier; our results support that, at least in a mouse model, the genetic background contributes to the integrity of the intestinal barrier during cholestasis.

Mounting evidence suggests that non-caspase proteases, in particular lysosomal cathepsins, are influential in the regulation of apoptosis.[50] Recently, B6 mice were found to have a natural cathepsin E deficiency compared with Balb/c and 129S2/Sv mice.[51] Cathepsin E is an aspartic endosomal proteinase, expressed at high levels in some epithelial and hematopoetic cells. The enzyme has been implicated in a variety of functions, including antigen processing.[52] Interestingly, we found that the B6 mice were deficient in cathepsin E in the intestine compared with A/J mice in sham-operated animals; however, that difference disappeared following CBDL as the cathepsin E expression increased in the ligated B6 mice. With no apparent strain differences in intestinal apoptosis or cathepsin E mRNA, our study suggests an apoptosis-independent mechanism may be responsible early on that then leads to the different outcomes seen later (3 weeks) following CBDL in the two strains. We speculate that apoptosis is increased in the intestine of ligated mice in both strains at time points greater than one week postoperatively. Recent evidence has shown that the host's innate immune response is regulated by the nuclear bile acid receptor, FXR, both in the small intestine[53] and colon.[54] We questioned whether differential FXR expression played a role in the strain differences noted in our CBDL model. We found no significant strain differences in FXR expression in either the jejunum or ileum.

Our Q-PCR data suggested two alternative mechanisms. The first candidate mechanism centered around claudin-2, known as a pore-forming tight junction; that is, claudin-2 expression

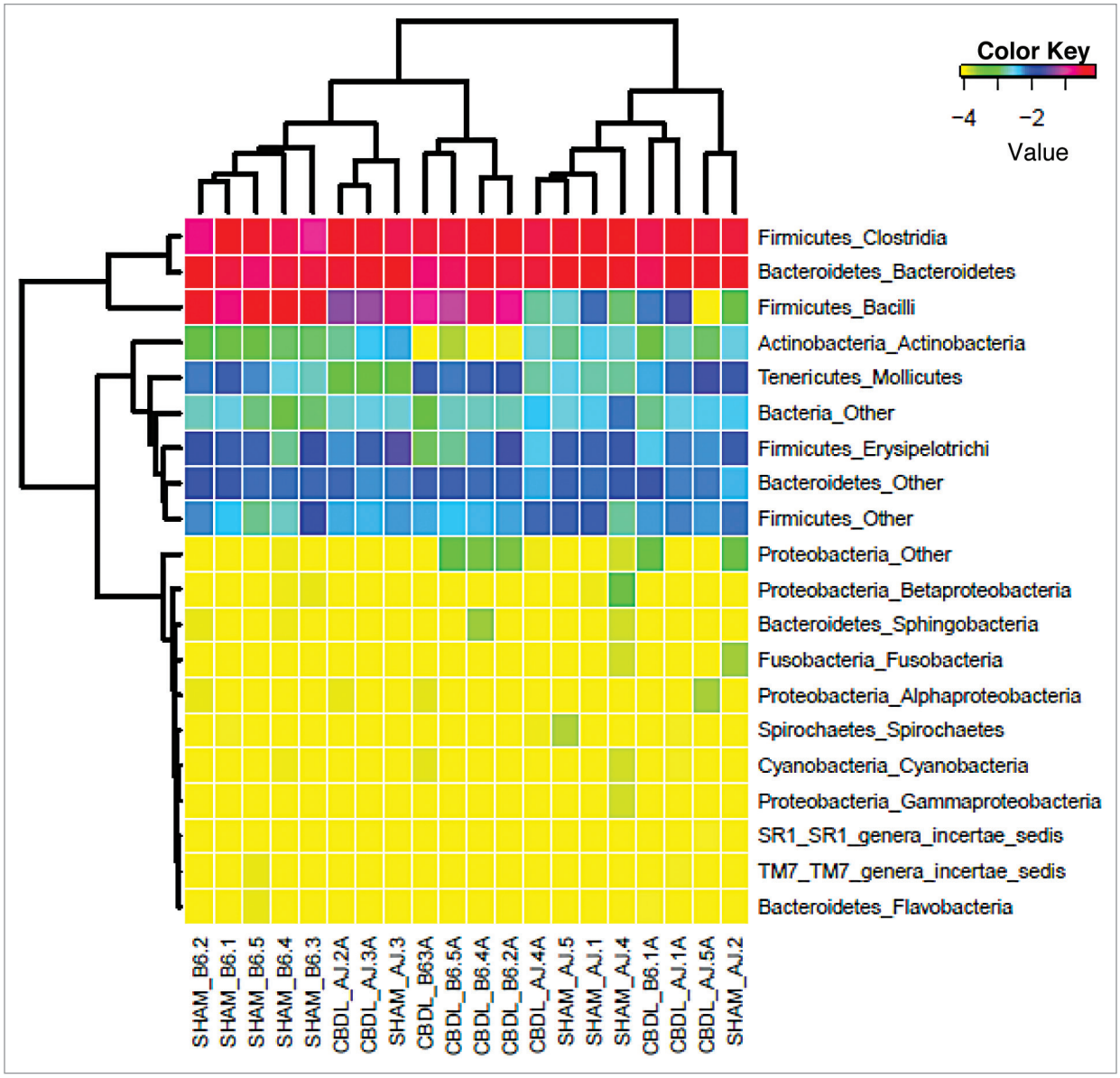

Figure 10. Heat map of classes of fecal microbiota collected from sham and ligated A/J and B6 mice (n = 5 mice for each of four groups). *Firmicutes* and *Bacteroidetes* dominate, as shown in red, but note the small increase in *Proteobacteria* following CBDL which was found in four of five B6 mice. This increase was not found in any of the ligated A/J mice.

correlates directly with "leakiness" of the gut.[55,56] The B6 mice demonstrated a strain-associated increase in claudin-2 mRNA expression compared with the A/J mice; however, the reverse was true regarding the protein, thus eliminating any significant role for this specific tight junction protein. The second possible mechanism suggested by our Q-PCR data are that increased IFN-γ and/or altered tight junction proteins may lead to the increased intestinal permeability and bacterial translocation found in the B6 mice. IFN-γ has been previously shown in vitro to disrupt epithelial barrier function by altering the architecture of the tight junction proteins, including a decrease in occludin expression.[22,24,25] In our study, we found increased IFN-γ mRNA as well as a reduction in occludin mRNA expression in ligated B6 mice. Furthermore, there appeared to be a trend toward decreased occludin protein expression in the B6 mice following a sham operation as compared with the A/J mice. Also, ZO-1 protein expression significantly decreased following CBDL in B6 but not A/J mice. This finding of increased IFN-γ expression with reduced ZO-1 levels is in agreement with in vitro work by Youakim et al.[25] Claudin-1 protein expression decreased significantly following CBDL in B6 mice but not A/J mice. Collectively, these alterations in the tight junction protein assembly may play an early role in the cascade of events leading to the worse outcome found several weeks following CBDL in B6 compared with A/J mice.

On the other hand, Sewnath et al.[34] demonstrated that endogenous IFN-γ was protective to the liver following cholestatic injury. They showed that IFN-γ receptor $(R)^{-/-}$ mice had a much lower

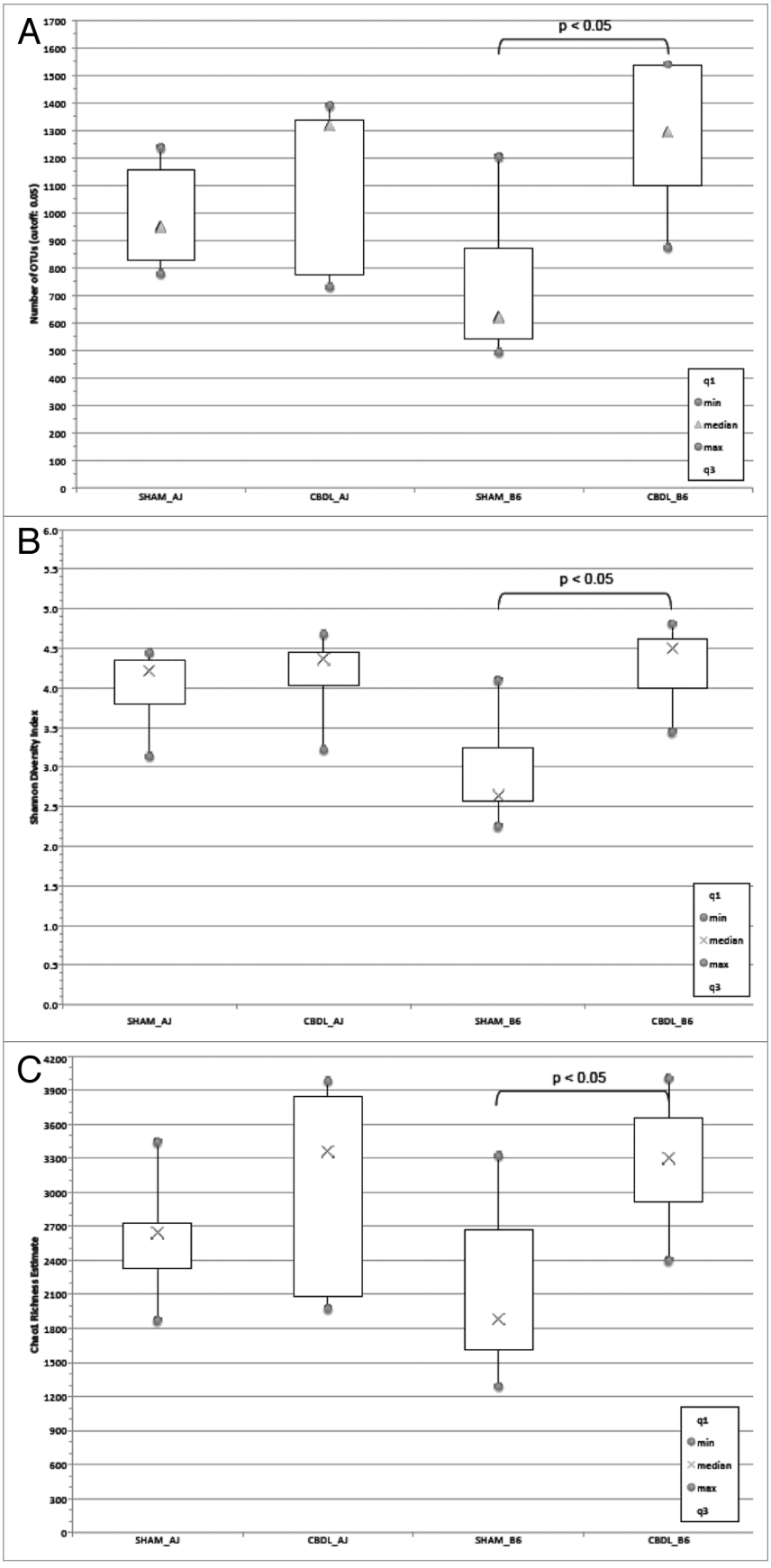

Figure 11. Diversity and richness of fecal Microbiota in sham and ligated A/J and B6 mice (n = 5 mice for each of four groups). (**A**) Sobs analysis of number of observed OTUs in A/J and B6 mice following Sham and CBDL procedures. Note that the number of fecal OTUs increases significantly in the B6 mice following CBDL as compared with shams, $p < 0.05$. There is no significant difference in the number of fecal OTUs in the A/J mice following CBDL as compared with shams. (**B**) Shannon diversity index analysis of A/J and B6 mice following sham and CBDL procedures. The B6 mice significantly increased their fecal bacterial diversity following CBDL compared with shams, $p < 0.05$. No significant difference was found in the A/J mice. (**C**) Chao1 richness estimate analysis of A/J and B6 mice following sham and CBDL procedures. B6 mice had a significantly elevated richness estimate of their fecal bacteria following CBDL compared with shams, $p < 0.05$. No significant difference was found in the A/J mice.

survival (40% mortality) two weeks following CBDL than the wild-type 129/Sv mice (0% mortality). Moreover, the IFN-γ $R^{-/-}$ mice had more severe jaundice and cholestatic liver injury reflected by higher serum bilirubin and liver enzyme levels as well as histology. Conversely, we hypothesized that a lack of IFN-γ would protect the intestine by preventing the decrease in occludin expression, increase TEER and improve survival. We found no mortality in either the IFN-$\gamma^{-/-}$ or the wild type B6 mice after two weeks of CBDL. Recognizing that the two studies used different strains of mice, we speculate that in our IFN-$\gamma^{-/-}$ (i.e., Not IFN-γ $R^{-/-}$) B6 mice, the lack of IFN-γ created greater intestinal resistance which offset the cholestatic liver injury to the point that the IFN-$\gamma^{-/-}$ mortality was not significantly increased compared with the wild-type. We posit that cholestasis is a complex pathologic condition in which the liver and intestinal injuries are precisely interrelated.

Following one week of CBDL, we expected to see increased intestinal mucosal atrophy evidenced by decreased villus/crypt ratios in ligated mice compared with sham controls. In addition, we expected to see more atrophic changes in the B6 strain; however, we found no significant histologic changes at seven days post-CBDL. Others have shown intestinal atrophy following seven days of CBDL in another rodent species, rats.[57] The ligated mice did demonstrate dilated lymphatics and edema in the lamina propria as previously reported in the literature;[48] however, there were no apparent strain differences. The lack of gross histologic changes may not be too surprising, given that apoptosis did not increase in the intestine in our

mice following one week of CBDL. In retrospect, we believe our time point was too premature to demonstrate the gross pathology seen following CBDL.

In summary, our study in A/J and B6 mice demonstrates that the intestinal barrier varies with each mouse strain. Whereas, we had hypothesized that the genetic background modulates the intestinal barrier following cholestatic injury; in fact, we found that the genetic background modulates the intestinal barrier at baseline (after a sham operation) as well as after CBDL. This was evidenced by the low baseline intestinal resistance and low expression of the tight junction protein, occludin, in the B6 mice. Following CBDL, the occludin and claudin-1 protein expression and TEER significantly decrease in each strain, such that the resistance in the ligated B6 mice remains significantly lower than that in the ligated A/J mice. We speculate that this very low resistance corresponds to a threshold being crossed, after which bacterial translocation and mortality later significantly increase in the B6 strain, which were also noted in our study. These differences support the notion that failure of the intestinal barrier in cholestatic mice results in increased episodes of sepsis and higher mortality. This study provides in vivo support for the apoptosis-independent mechanism of IFN-γ mediated disruption of the intestinal barrier. In addition, our study showed that the genetic background of the host influenced the gut microbiota and resulted in a dysbiosis following CBDL in one strain. Notably, this dysbiosis was positively correlated with the strain-dependent increase in mortality later seen following CBDL. This altered microbiota may play a causal role in the pathologic changes following CBDL. The genetic differences noted in these two strains of mice may extrapolate to human variations and potentially provide a basis for identifying individuals at risk for exaggerated injury following cholestasis. Furthermore, alterations in the intestinal microbiota via prebiotics, probiotics or symbiotics may have therapeutic implications in the treatment of cholestatic patients in the future.

Materials and Methods

Animals. Male A/J and C57BL/6J (B6) and IFN-$\gamma^{-/-}$ (B6 background) mice (8 weeks old) were obtained from the Jackson Laboratory and maintained in identical environmental conditions with identical diets in a pathogen-free animal facility with 12-h light-dark cycles. All mice weighed 18 to 25 g at the time of operation. Animal studies were conducted according to protocols reviewed and approved by the University of Maryland School of Medicine Institutional Animal Care and Use Committee and adhered to guidelines promulgated by the National Institutes of Health.

CBDL operative procedure. Mice were anesthetized by inhaled isoflurane anesthesia. The abdomen was clipped and then prepared in sterile fashion with 70% ethyl-ethanol followed by betadine. A transverse upper abdominal incision was performed. The CBD was dissected away from the portal vein and was ligated near its junction with the duodenum using aneurysm clips engineered with a precisely standardized opening and closing mechanism. The abdominal wall was then closed in a two-layer fashion using absorbable sutures. Sham-operated mice were treated identically but without dissection or ligation of the CBD. Postoperatively, animals were resuscitated with warmed subcutaneous injections of saline (1 mL) to replace losses. Mice were returned to clean cages where food and water were provided ad libitum.

Histology. Seven days after CBDL or sham operation, mice underwent anesthesia with isoflurane and euthanasia by cervical dislocation. Their previous incision was reopened and the small intestine was resected. Jejunal and ileal sections were pinned to preserve their architecture and then placed in 4% paraformaldehyde, paraffin-embedded and cut into 5 μm-thick sections. Sections were stained with hematoxylin and eosin for determination of histopathological features, including villus height, crypt depth, inflammation, dilatation of lacteals and edema in the lamina propria. Three weeks after CBDL, mice underwent the same histologic protocol; however this time, the specimens were lung, liver, kidney and heart tissue. Inflammation manifesting as neutrophil infiltration and/or edema was noted and served as a marker for systemic sepsis.

Apoptosis. Seven days following CBDL, apoptosis was determined using a TUNEL assay performed with a commercially available kit, according to manufacturer specifications (Millipore). In addition, apoptosis was also measured by evaluating the crypt cells for pyknosis and karyorrhexis. Apoptosis was quantified in 100 crypts from well-oriented crypt-villus units, defined as a crypt sectioned parallel to the crypt-villus axis with Paneth cells at the crypt base and an unbroken epithelial column extending to the villus tip.[30] The slides were reviewed by a pathologist who was blinded to the treatment assignments.

Transepithelial electrical resistance (TEER), Ussing chambers and FITC-dextran intestinal permeability. We used a modified snap-well assay system described by El Asmar et al.[31] to measure TEER of the intestinal mucosa. Briefly, seven days following CBDL or sham operation, segments of the jejunum were resected and the muscle layers carefully stripped away from the mucosa. For each mouse, three 0.07 cm^2 pieces of mucosa were mounted in snap-well chambers (Costar) and cultured in DMEM without serum. Epithelial resistance was measured every 30 min using an EndOhm-24 and EVOM voltmeter (World Precision Instrument). Intestinal tissue permeability was also assessed in our TEER snapwells using a FITC-Dextran assay. Briefly, muscle-free jejunal samples were mounted in snapwells with the mucosal side up. 4-kDa FITC-Dextran in D-MEM pre-warmed at 37°C was placed in the top compartment of each well, and samples were collected over time from the bottom compartment of each well. A sample from the top compartment at the time of the last sampling of the bottom compartment was used to normalize the samples to account for possible differences in the total fluorescence added at the beginning of the experiment. Fluorescence of the samples was quantified in a multi-plate fluorescence reader in black 96 well plates; excitation wavelength was 485 nm and emission wavelength was 538 nm.

To confirm our TEER results, resistance was also calculated from Ussing chambers. For each strain, four 1 cm segments of

mucosa were stripped of muscle and mounted in Ussing chambers that exposed 0.126 cm^2 to 10 ml of Kreb's buffer. Agar-salt bridges and electrodes were used to measure potential difference. Every 50 sec, the tissues were short-circuited at 1 V for 10 sec (World Precision Instruments DVC 1000 V clamp) to allow calculation of tissue resistance using Ohm's law.

Bacterial cultures. Our pilot experiments demonstrated that translocation, defined as a positive mesenteric lymph node culture, was a rare event after only one week of ligation, so we focused our efforts on translocation occurring after three weeks of ligation. This time point was physiologically relevant as evidenced by the signs of chronic obstructive jaundice, including ascites, which was seen in the majority of the mice. Twenty-one days after CBDL, separate groups of mice underwent anesthesia with isoflurane and euthanasia by cervical dislocation. Their thoraco-abdominal area was prepped with betadine. A median sternotomy was performed, and blood was collected by direct cardiac puncture. Their previous incision was reopened. Liver, spleen and mesenteric lymph nodes (MLNs) were resected. While maintaining sterile conditions, blood and the aforementioned tissue specimens were then plated onto blood agar plates and incubated for 24 h at 37°C. In order to ensure sterility and prevent cross contamination, we chose not to use a homogenizer; rather, the specimens were minced with sterile scissors. The plates were examined non-quantitatively for the presence of bacterial growth, and isolates were identified. Bacterial translocation was defined by the presence of bacteria on the agar plate.

Soluble CD14 measurement by ELISA. Soluble CD14 is a biomarker for monocyte activation following endotoxemia. Fourteen days following CBDL or sham operation, blood was collected. A commercially available enzyme-linked immunosorbent assay was used according to the manufacturer's protocol for measuring soluble CD14 (biometec).

RNA extraction, cDNA synthesis and real-time quantitative PCR (Q-PCR) analysis. Seven days following CBDL or sham operation, intestine was harvested. Total RNA was isolated from homogenized jejunal samples that were stored in TRIzol (Invitrogen). The total RNA was isolated from TRIzol samples as per the manufacturer's instructions. The pellet was allowed to air-dry, and the total RNA was resuspended in an appropriate volume of RNase-free water. RNA concentrations were calculated using a NanoDrop 1000 spectrophotometer (Thermo Scientific). Single stranded cDNA was synthesized from 2 μg of total RNA using random hexamer primer and the First Strand cDNA Synthesis Kit (MBI Fermentas). The specific primer sequences were designed using Beacon Designer 7.0 (Premier Biosoft International) and synthesized by the University of Maryland School of Medicine Biopolymer/Genomics Core. Q-PCR reactions were set up using iQ SYBR Green Supermix (Bio-Rad) in a total volume of 25 μl. Amplification conditions were: 95°C for 3 min, 50 cycles of 95°C for 15 sec, 60°C for 15 sec and 72°C for 20 sec. All reactions were performed using Bio-Rad iCycler instrumentation and software. All samples were normalized with 18s rRNA housekeeping gene levels with subsequent calculation of fold-change in mRNA expression. Analysis was performed in GraphPad Prism5.

Western blot analysis of tight junction proteins. Expression of claudin-1, claudin-2, occludin and zona occludins-1 (ZO-1) were quantified by western blot analysis. The antibodies recognizing occludin and ZO-1 were obtained from Invitrogen (Grand Island, NY). Claudin-1 and claudin-2 antibodies were purchased from Santa Cruz Biotechnology. Fluorescein-conjugated goat anti-mouse and goat anti-rabbit antibodies were purchased from Santa Cruz Biotechnology. Briefly, 1-cm sections of mid-jejunal intestine were harvested from each mouse and immediately homogenized in 1 mL ice-cold RIPA-buffer (50 mM TRIS-HCl, pH 7.4, 150 mM NaCl, 1 mM DTT, 0.5 mM EDTA, 1.0% NP40, 0.5% sodium deoxycholate, 0.1% SDS, 2 mM phenylmethylsulfonyl fluoride, 20 μg/ml aprotinin, 2 μg/ml leupeptin and 2 mM sodium orthovanadate). Tissue lysates were sonicated, incubated on ice for 20 min and centrifuged at 4°C; supernatants were subsequently collected for immunoprecipitation. The protein concentration of the supernatants was measured using the technique previously described by Bradford.[32] Following 5 min of boiling samples, equal amounts of protein (2 μg) were loaded into each lane and protein was subjected to electrophoresis on 10% acrylamide gels. Following the transfer of protein onto nitrocellulose filters, they were incubated with primary antibodies directed against occludin, claudin-1 and ZO-1 overnight at 4°C. The filters were subsequently washed with 1 × TBST and incubated with secondary antibodies conjugated with horseradish peroxidase (HRP) for one hour at room temperature. Following this, immunocomplexes were detected by chemiluminescence.

Gut bacterial community profiling using 454 pyrosequencing of the 16S rRNA gene. After being housed under identical environmental conditions, including diet, A/J and B6 mice underwent either a sham (n = 5 A/J and 5 C57BL/6J) or CBDL (n = 5 A/J and 5 C57BL/6J) operation. Two weeks later, their stool was collected. Profiling of the bacterial communities inhabiting the gut of Male A/J and C57BL/6J (B6) was performed as previously described.[33] Total genomic DNA was extracted from fecal pellets using the protocol described by Zupancic and colleagues. Briefly, 1 ml of phosphate-buffered saline was added to the mouse stool aliquots and cell lysis was performed using an enzymatic cocktail composed of lyzosyme, mutanolysin and lysostaphin. After one hour of incubation at 37°C, samples were further lysed by addition of proteinase K and 10% SDS, followed by incubation at 55°C for 45 min. The samples were then disrupted by bead beating using a FP120 FastPrep instrument and 0.1 mm silica spheres. The resulting crude lysate was processed using the ZYMO Fecal DNA Kit (Zymogen) according to the manufacturer's recommendations. Negative extraction controls, where stool samples were omitted, were performed to ensure the samples were not contaminated by exogenous bacterial DNA during the extraction process.

The universal primers 27F and 338R were then used for PCR amplification of the V1–V3 hypervariable regions of 16S rRNA genes. The 338R primer included a unique sequence tag to barcode each sample. Using 96 barcoded 338R primers, the V1–V3 regions of 16S rRNA genes were amplified in 96-well microtiter plates using AmpliTaq Gold DNA polymerase (Applied Biosystems) and 50 ng of template DNA in a total reaction

volume of 50 mL, using the cycling conditions described by Zupancic and colleagues.[33] Negative controls without a template were included for each barcoded primer pair. PCR products were quantified using the Quant-iT PicoGreen dsDNA assay, and equimolar amounts (100 ng) of the PCR amplicons were mixed in a single tube. The purified amplicon mixture was then sequenced by 454 FLX Titanium pyrosequencing using 454 Life Sciences primer A by the Genomics Resource Center at the Institute for Genome Sciences, University of Maryland School of Medicine, using protocols recommended by the manufacturer as amended by the Center. Processing (sequence binning and trimming) and analysis of the 16S rRNA reads was performed using the CLoVR system (CloVR 1.0-RC2; http://clovr.org/) and the CloVR-16S protocol (http://clovr.org/methods/clovr-16s; version 1.1).

Statistical analysis. ANOVA was used to determine significance in the TEER data. For the bacterial translocation experiments and the mortality study, a two-sided Fisher's exact test was used. Statistical probability of $p < 0.05$ was considered significant. Q-PCR data was analyzed using ANOVA with the Bonferroni post-test.

Disclosure of Potential Conflicts of Interest

No potential conflict of interest was disclosed.

Acknowledgments

Research reported in this publication was supported by the National Institute of General Medical Sciences of the National Institutes of Health under award number K08GM081701. The content is solely the responsibility of the authors and does not necessarily represent the official views of the National Institutes of Health.

References

1. De Maio A, Torres MB, Reeves RH. Genetic determinants influencing the response to injury, inflammation, and sepsis. Shock 2005; 23:11-7; PMID:15614125; http://dx.doi.org/10.1097/01.shk.0000144134.03598.c5.
2. De Maio A, Mooney ML, Matesic LE, Paidas CN, Reeves RH. Genetic component in the inflammatory response induced by bacterial lipopolysaccharide. Shock 1998; 10:319-23; PMID:9840645; http://dx.doi.org/10.1097/00024382-199811000-00002.
3. Stewart D, Fulton WB, Wilson C, Monitto CL, Paidas CN, Reeves RH, et al. Genetic contribution to the septic response in a mouse model. Shock 2002; 18:342-7; PMID:12392278; http://dx.doi.org/10.1097/00024382-200210000-00009.
4. Nishikawa F, Yoshikawa S, Harada H, Kita M, Kita E. The full expression of the ity phenotype in ityr mice requires C3 activation by Salmonella lipopolysaccharide. Immunology 1998; 95:640-7; PMID:9893057; http://dx.doi.org/10.1046/j.1365-2567.1998.00647.x.
5. Banus HA, Vandebriel RJ, de Ruiter H, Dormans JA, Nagelkerke NJ, Mooi FR, et al. Host genetics of Bordetella pertussis infection in mice: significance of Toll-like receptor 4 in genetic susceptibility and pathobiology. Infect Immun 2006; 74:2596-605; PMID:16622195; http://dx.doi.org/10.1128/IAI.74.5.2596-2605.2006.
6. Tuite A, Elias M, Picard S, Mullick A, Gros P. Genetic control of susceptibility to Candida albicans in susceptible A/J and resistant C57BL/6J mice. Genes Immun 2005; 6:672-82; PMID:16079897.
7. Hernandez-Valladares M, Naessens J, Nagda S, Musoke AJ, Rihet P, Ole-Moiyoi OK, et al. Comparison of pathology in susceptible A/J and resistant C57BL/6J mice after infection with different sub-strains of Plasmodium chabaudi. Exp Parasitol 2004; 108:134-41; PMID:15582510; http://dx.doi.org/10.1016/j.exppara.2004.07.011.
8. Czuprynski CJ, Faith NG, Steinberg H. A/J mice are susceptible and C57BL/6 mice are resistant to Listeria monocytogenes infection by intragastric inoculation. Infect Immun 2003; 71:682-9; PMID:12540546; http://dx.doi.org/10.1128/IAI.71.2.682-689.2003.
9. Hughes MA, Green CS, Lowchyj L, Lee GM, Grippe VK, Smith MF Jr., et al. MyD88-dependent signaling contributes to protection following Bacillus anthracis spore challenge of mice: implications for Toll-like receptor signaling. Infect Immun 2005; 73:7535-40; PMID:16239556; http://dx.doi.org/10.1128/IAI.73.11.7535-7540.2005.
10. Georgiev P, Jochum W, Heinrich S, Jang JH, Nocito A, Dahm F, et al. Characterization of time-related changes after experimental bile duct ligation. Br J Surg 2008; 95:646-56; PMID:18196571; http://dx.doi.org/10.1002/bjs.6050.
11. Alaish SM, Torres M, Ferlito M, Sun CC, De Maio A. The severity of cholestatic injury is modulated by the genetic background. Shock 2005; 24:412-6; PMID:16247325; http://dx.doi.org/10.1097/01.shk.0000183392.83272.97.
12. Hollander D. Crohn's disease--a permeability disorder of the tight junction? Gut 1988; 29:1621-4; PMID:3065154; http://dx.doi.org/10.1136/gut.29.12.1621.
13. Murphy MS, Eastham EJ, Nelson R, Pearson AD, Laker MF. Intestinal permeability in Crohn's disease. Arch Dis Child 1989; 64:321-5; PMID:2495775; http://dx.doi.org/10.1136/adc.64.3.321.
14. Hollander D, Vadheim CM, Brettholz E, Petersen GM, Delahunty T, Rotter JI. Increased intestinal permeability in patients with Crohn's disease and their relatives. A possible etiologic factor. Ann Intern Med 1986; 105:883-5; PMID:3777713; http://dx.doi.org/10.7326/0003-4819-105-6-883.
15. Pascual S, Such J, Esteban A, Zapater P, Casellas JA, Aparicio JR, et al. Intestinal permeability is increased in patients with advanced cirrhosis. Hepatogastroenterology 2003; 50:1482-6; PMID:14571769.
16. Campillo B, Pernet P, Bories PN, Richardet JP, Devanlay M, Aussel C. Intestinal permeability in liver cirrhosis: relationship with severe septic complications. Eur J Gastroenterol Hepatol 1999; 11:755-9; PMID:10445796; http://dx.doi.org/10.1097/00042737-199907000-00013.
17. Li Q, Zhang Q, Wang C, Liu X, Li N, Li J. Disruption of tight junctions during polymicrobial sepsis *in vivo*. J Pathol 2009; 218:210-21; PMID:19235836; http://dx.doi.org/10.1002/path.2525.
18. Zhou P, Li E, Shea-Donohue T, Singer SM. Tumour necrosis factor α contributes to protection against Giardia lamblia infection in mice. Parasite Immunol 2007; 29:367-74; PMID:17576366; http://dx.doi.org/10.1111/j.1365-3024.2007.00953.x.
19. Hyun CS, Chen CW, Shinowara NL, Palaia T, Fallick FS, Martello LA, et al. Morphological factors influencing transepithelial conductance in a rabbit model of ileitis. Gastroenterology 1995; 109:13-23; PMID:7797012; http://dx.doi.org/10.1016/0016-5085(95)90264-3.
20. Pérez-Paramo M, Muñoz J, Albillos A, Freile I, Portero F, Santos M, et al. Effect of propranolol on the factors promoting bacterial translocation in cirrhotic rats with ascites. Hepatology 2000; 31:43-8; PMID:10613726; http://dx.doi.org/10.1002/hep.510310109.
21. Clayburgh DR, Shen L, Turner JR. A porous defense: the leaky epithelial barrier in intestinal disease. Lab Invest 2004; 84:282-91; PMID:14767487; http://dx.doi.org/10.1038/labinvest.3700050.
22. Madara JL, Stafford J. Interferon-gamma directly affects barrier function of cultured intestinal epithelial monolayers. J Clin Invest 1989; 83:724-7; PMID:2492310; http://dx.doi.org/10.1172/JCI113938.
23. Marano CW, Lewis SA, Garulacan LA, Soler AP, Mullin JM. Tumor necrosis factor-alpha increases sodium and chloride conductance across the tight junction of CACO-2 BBE, a human intestinal epithelial cell line. J Membr Biol 1998; 161:263-74; PMID:9493132; http://dx.doi.org/10.1007/s002329900333.
24. Bruewer M, Luegering A, Kucharzik T, Parkos CA, Madara JL, Hopkins AM, et al. Proinflammatory cytokines disrupt epithelial barrier function by apoptosis-independent mechanisms. J Immunol 2003; 171:6164-72; PMID:14634132.
25. Youakim A, Ahdieh M. Interferon-gamma decreases barrier function in T84 cells by reducing ZO-1 levels and disrupting apical actin. Am J Physiol 1999; 276:G1279-88; PMID:10330020.
26. Berg RD, Garlington AW. Translocation of certain indigenous bacteria from the gastrointestinal tract to the mesenteric lymph nodes and other organs in a gnotobiotic mouse model. Infect Immun 1979; 23:403-11; PMID:154474.
27. Runyon BA, Squier S, Borzio M. Translocation of gut bacteria in rats with cirrhosis to mesenteric lymph nodes partially explains the pathogenesis of spontaneous bacterial peritonitis. J Hepatol 1994; 21:792-6; PMID:7890896; http://dx.doi.org/10.1016/S0168-8278(94)80241-6.
28. Garcia-Tsao G, Lee FY, Barden GE, Cartun R, West AB. Bacterial translocation to mesenteric lymph nodes is increased in cirrhotic rats with ascites. Gastroenterology 1995; 108:1835-41; PMID:7768390; http://dx.doi.org/10.1016/0016-5085(95)90147-7.
29. Llovet JM, Bartolí R, March F, Planas R, Viñado B, Cabré E, et al. Translocated intestinal bacteria cause spontaneous bacterial peritonitis in cirrhotic rats: molecular epidemiologic evidence. J Hepatol 1998; 28:307-13; PMID:9580278; http://dx.doi.org/10.1016/0168-8278(88)80018-7.
30. Coopersmith CM, Stromberg PE, Dunne WM, Davis CG, Amiot DM 2nd, Buchman TG, et al. Inhibition of intestinal epithelial apoptosis and survival in a murine model of pneumonia-induced sepsis. JAMA 2002; 287:1716-21; PMID:11926897; http://dx.doi.org/10.1001/jama.287.13.1716.

31. El Asmar R, Panigrahi P, Bamford P, Berti I, Not T, Coppa GV, et al. Host-dependent zonulin secretion causes the impairment of the small intestine barrier function after bacterial exposure. Gastroenterology 2002; 123:1607-15; PMID:12404235; http://dx.doi.org/10.1053/gast.2002.36578.
32. Bradford MM. A rapid and sensitive method for the quantitation of microgram quantities of protein utilizing the principle of protein-dye binding. Anal Biochem 1976; 72:248-54; PMID:942051; http://dx.doi.org/10.1016/0003-2697(76)90527-3.
33. Zupancic ML, Cantarel BL, Liu Z, Drabek EF, Ryan KA, Cirimotich S, et al. Analysis of the gut microbiota in the old order Amish and its relation to the metabolic syndrome. PLoS One 2012; 7:e43052; PMID:22905200; http://dx.doi.org/10.1371/journal.pone.0043052.
34. Sewnath ME, Van Der Poll T, Van Noorden CJF, Ten Kate FJ, Gouma DJ. Endogenous interferon γ protects against cholestatic liver injury in mice. Hepatology 2002; 36:1466-77; PMID:12447873.
35. Rees LE, Cogan TA, Dodson AL, Birchall MA, Bailey M, Humphrey TJ. Campylobacter and IFNgamma interact to cause a rapid loss of epithelial barrier integrity. Inflamm Bowel Dis 2008; 14:303-9; PMID:18050297; http://dx.doi.org/10.1002/ibd.20325.
36. Köhler H, Sakaguchi T, Hurley BP, Kase BA, Reinecker HC, McCormick BA. Salmonella enterica serovar Typhimurium regulates intercellular junction proteins and facilitates transepithelial neutrophil and bacterial passage. Am J Physiol Gastrointest Liver Physiol 2007; 293:G178-87; PMID:17615177; http://dx.doi.org/10.1152/ajpgi.00535.2006.
37. Howe KL, Reardon C, Wang A, Nazli A, McKay DM. Transforming growth factor-beta regulation of epithelial tight junction proteins enhances barrier function and blocks enterohemorrhagic Escherichia coli O157:H7-induced increased permeability. Am J Pathol 2005; 167:1587-97; PMID:16314472; http://dx.doi.org/10.1016/S0002-9440(10)61243-6.
38. Yang R, Harada T, Li J, Uchiyama T, Han Y, Englert JA, et al. Bile modulates intestinal epithelial barrier function via an extracellular signal related kinase 1/2 dependent mechanism. Intensive Care Med 2005; 31:709-17; PMID:15782315; http://dx.doi.org/10.1007/s00134-005-2601-9.
39. Wells CL, Hess DJ, Erlandsen SL. Impact of the indigenous flora in animal models of shock and sepsis. Shock 2004; 22:562-8; PMID:15545829; http://dx.doi.org/10.1097/01.shk.0000145935.24344.2d.
40. Ley RE, Bäckhed F, Turnbaugh P, Lozupone CA, Knight RD, Gordon JI. Obesity alters gut microbial ecology. Proc Natl Acad Sci U S A 2005; 102:11070-5; PMID:16033867; http://dx.doi.org/10.1073/pnas.0504978102.
41. Fouts DE, Torralba M, Nelson KE, Brenner DA, Schnabl B. Bacterial translocation and changes in the intestinal microbiome in mouse models of liver disease. J Hepatol 2012; 56:1283-92; PMID:22326468; http://dx.doi.org/10.1016/j.jhep.2012.01.019.
42. Turnbaugh PJ, Ley RE, Mahowald MA, Magrini V, Mardis ER, Gordon JI. An obesity-associated gut microbiome with increased capacity for energy harvest. Nature 2006; 444:1027-31; PMID:17183312; http://dx.doi.org/10.1038/nature05414.
43. Turnbaugh PJ, Bäckhed F, Fulton L, Gordon JI. Diet-induced obesity is linked to marked but reversible alterations in the mouse distal gut microbiome. Cell Host Microbe 2008; 3:213-23; PMID:18407065; http://dx.doi.org/10.1016/j.chom.2008.02.015.
44. Cani PD, Amar J, Iglesias MA, Poggi M, Knauf C, Bastelica D, et al. Metabolic endotoxemia initiates obesity and insulin resistance. Diabetes 2007; 56:1761-72; PMID:17456850; http://dx.doi.org/10.2337/db06-1491.
45. Cani PD, Bibiloni R, Knauf C, Waget A, Neyrinck AM, Delzenne NM, et al. Changes in gut microbiota control metabolic endotoxemia-induced inflammation in high-fat diet-induced obesity and diabetes in mice. Diabetes 2008; 57:1470-81; PMID:18305141; http://dx.doi.org/10.2337/db07-1403.
46. Azcarate-Peril MA, Foster DM, Cadenas MB, Stone MR, Jacobi SK, Stauffer SH, et al. Acute necrotizing enterocolitis of preterm piglets is characterized by dysbiosis of ileal mucosa-associated bacteria. Gut Microbes 2011; 2:234-43; PMID:21983069; http://dx.doi.org/10.4161/gmic.2.4.16332.
47. Mai V, Young CM, Ukhanova M, Wang X, Sun Y, Casella G, et al. Fecal microbiota in premature infants prior to necrotizing enterocolitis. PLoS One 2011; 6:e20647; PMID:21674011; http://dx.doi.org/10.1371/journal.pone.0020647.
48. Deitch EA, Sittig K, Li M, Berg R, Specian RD. Obstructive jaundice promotes bacterial translocation from the gut. Am J Surg 1990; 159:79-84; PMID:2136788; http://dx.doi.org/10.1016/S0002-9610(05)80610-5.
49. Slocum MM, Sittig KM, Specian RD, Deitch EA. Absence of intestinal bile promotes bacterial translocation. Am Surg 1992; 58:305-10; PMID:1622012.
50. Conus S, Simon HU. Cathepsins: key modulators of cell death and inflammatory responses. Biochem Pharmacol 2008; 76:1374-82; PMID:18762176; http://dx.doi.org/10.1016/j.bcp.2008.07.041.
51. Tulone C, Tsang J, Prokopowicz Z, Grosvenor N, Chain B. Natural cathepsin E deficiency in the immune system of C57BL/6J mice. Immunogenetics 2007; 59:927-35; PMID:18000662; http://dx.doi.org/10.1007/s00251-007-0256-0.
52. Bennett K, Levine T, Ellis JS, Peanasky RJ, Samloff IM, Kay J, et al. Antigen processing for presentation by class II major histocompatibility complex requires cleavage by cathepsin E. Eur J Immunol 1992; 22:1519-24; PMID:1601038; http://dx.doi.org/10.1002/eji.1830220626.
53. Inagaki T, Moschetta A, Lee YK, Peng L, Zhao G, Downes M, et al. Regulation of antibacterial defense in the small intestine by the nuclear bile acid receptor. Proc Natl Acad Sci U S A 2006; 103:3920-5; PMID:16473946.
54. Vavassori P, Mencarelli A, Renga B, Distrutti E, Fiorucci SJ. The bile acid receptor FXR is a modulator of intestinal innate immunity. Immunol 2009; 183:6251-61; http://dx.doi.org/10.4049/jimmunol.0803978.
55. Zeissig S, Bürgel N, Günzel D, Richter J, Mankertz J, Wahnschaffe U, et al. Changes in expression and distribution of claudin 2, 5 and 8 lead to discontinuous tight junctions and barrier dysfunction in active Crohn's disease. Gut 2007; 56:61-72; PMID:16822808; http://dx.doi.org/10.1136/gut.2006.094375.
56. Amasheh M, Grotjohann I, Amasheh S, Fromm A, Soderholm JD, Zeitz M, et al. Regulation of mucosal structure and barrier function in rat colon exposed to tumor necrosis factor alpha and interferon gamma in vitro: A novel model for studying the pathomechanisms of inflammatory bowel disease cytokines. Scand J Gastroenterol 2009; 4:1-10; PMID:19658020.
57. Sabuncuoglu MZ, Kismet K, Kilicoglu SS, Kilicoglu B, Erel S, Muratoglu S, et al. Propolis reduces bacterial translocation and intestinal villus atrophy in experimental obstructive jaundice. World J Gastroenterol 2007; 13:5226-31; PMID:17876893.